

# Forward dispersion relations and Roy equations in $\pi\pi$ scattering

R. Kamiński<sup>1</sup>, J.R. Peláez<sup>2,a</sup>, and F.J. Ynduráin<sup>3</sup>

<sup>1</sup> Department of Theoretical Physics Henryk Niewodniczański Institute of Nuclear Physics, Polish Academy of Sciences, 31-242, Kraków, Poland

<sup>2</sup> Departamento de Física Teórica, II (Métodos Matemáticos), Facultad de Ciencias Físicas, Universidad Complutense de Madrid, E-28040, Madrid, Spain

<sup>3</sup> Departamento de Física Teórica, C-XI Universidad Autónoma de Madrid, Canto Blanco, E-28049, Madrid, Spain

Received: 8 January 2007

Published online: 27 March 2007 – © Società Italiana di Fisica / Springer-Verlag 2007

**Abstract.** We first review the results of an analysis of  $\pi\pi$  interactions in  $S$ ,  $P$  and  $D$  waves for the two-pion effective mass from threshold to about 1.4 GeV. In particular, we show a recent improvement of this analysis above the  $K\bar{K}$  threshold using more data for phase shifts and including the  $S0$ -wave inelasticity from  $\pi\pi \rightarrow K\bar{K}$ . In addition, we have improved the fit to the  $f_2(1270)$ -resonance and used a more flexible  $P$ -wave parametrization above the  $K\bar{K}$  threshold and included an estimation of the  $D2$ -wave inelasticity. The better accuracy thus achieved also required a refinement of the Regge analysis above 1.42 GeV. Finally, in this work we check that the  $\pi\pi$  scattering amplitudes obtained in this approach satisfy remarkably well forward dispersion relations and Roy's equations.

**PACS.** 13.75.Lb Meson-meson interactions

## 1 Introduction

In a previous analysis [1] a set of fits to different data sets on  $\pi\pi$  scattering was presented together with a detailed description of the mathematical methods used in calculations. Forward dispersion relations (FDRs) were then used in order to test the correctness of the amplitudes thus constructed. Remarkably, it was found that some of the very frequently used sets of phase shifts do not satisfy FDRs below 1 GeV. Thus, FDRs were shown to give strong constraints to fits which, when used later as a constraint, lead to an improved and precise representation of  $\pi\pi$  scattering amplitudes below, roughly 1 GeV. In the regions from about 1 GeV to 1.4 GeV there was still some mismatch between the real part of the amplitudes and the results of dispersive evaluations in [1] (especially for  $\pi^0\pi^0$  scattering).

In a subsequent article [2], in order to improve the agreement with the constraints given by FDRs, we have reanalysed the parametrizations of the  $S0$  above  $K\bar{K}$  threshold, the  $D0$ -wave and, to a lesser extent, the  $P$  and  $D2$  waves. In the  $S0$ -wave we took into account systematically the elasticity data from the  $\pi\pi \rightarrow K\bar{K}$  reaction [3–7], included in the fit more data on phase shifts above the  $K\bar{K}$  threshold [3–6] and used a more flexible parametrization from 0.932 GeV to 1.4 GeV. In the  $D0$ -wave we have used experimental data from [3, 6, 8], information on low-energy parameters (the scattering length and slope) and included in the fit the width and mass of the  $f_2(1270)$ -resonance as

given by the PDG [9]. The result is that, for both  $S0$  and  $D0$  waves, we have obtained more accurate parametrizations with smaller errors compared to those in the previous approach [1]. In the  $P$ -wave we have exploited a more flexible parametrization between the  $K\bar{K}$  threshold and 1.42 GeV and in the  $D2$ -wave we have included its estimated inelasticity above 1 GeV.

This more accurate determination of the  $\pi\pi$  amplitudes below 1.42 GeV allowed us to refine the Regge analysis that had been used in [1, 10]. This has been done by removing the degeneracy condition  $\alpha_\rho(0) = \alpha_{\rho'}(0)$  which thus modifies slightly the central values of the intercepts  $\alpha_\rho(0)$  (by  $\sim 11\%$ ) and  $\alpha_{\rho'}(0)$  (by  $\sim 4\%$ ), but yields smaller errors than those in [1].

We have found that the  $\pi\pi$  amplitudes with the new parametrizations of phase shifts and inelasticities in the  $S$ ,  $P$  and  $D$  waves together with the just discussed small changes in  $\alpha_\rho(0)$  and  $\alpha_{\rho'}(0)$  allow for a much better fulfilment of FDRs than in [1]. The biggest improvement in  $\chi^2$  (about 66%) is achieved for the forward  $\pi^0\pi^0$  dispersion relation and a smaller one (about 15%) for  $\pi^0\pi^+$ . In the case of the forward dispersion relation for isopin 1 in the  $t$ -channel a very tiny deterioration has been found ( $\chi^2$  increased by about 26%), which is still acceptable, since, considering all FDRs together, there is a considerable overall improvement in their fulfilment. It is worth noting that this has been achieved despite the improved data fits have smaller errors than in [1].

Finally, in the present work, and using those improved parametrizations, we will test the Roy equations, which,

<sup>a</sup> e-mail: jrpelaez@fis.ucm.es

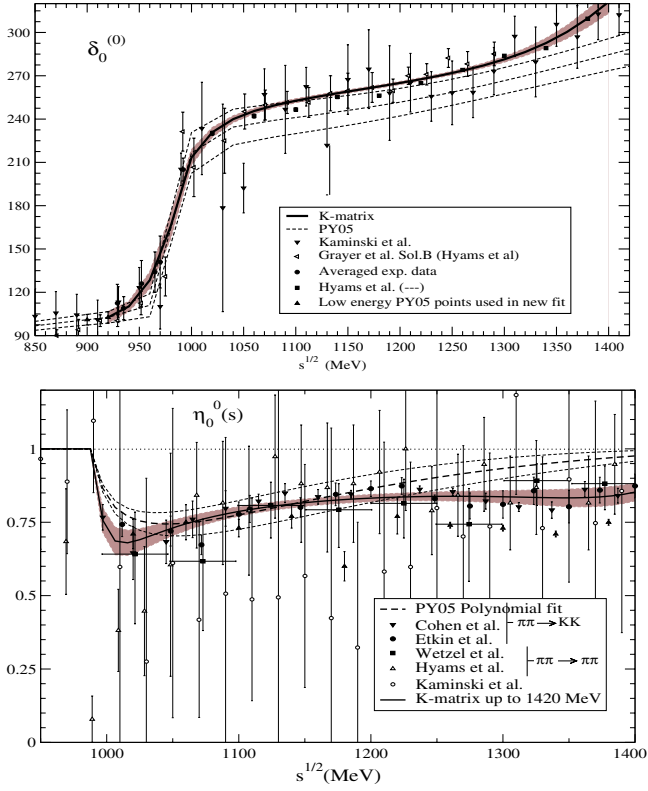


**Fig. 1.** Phase shifts and inelasticities of the  $S_0$ -wave fitted using the  $\mathbf{K}$ -matrix approach of [2] (solid lines). The dotted lines represent the results of [1].

contrary to FDRs, incorporate  $s$ - $t$  crossing, by calculating the difference between the real parts of the input amplitudes and those obtained from Roy's equations. We have found that, on average, and up to almost the  $K\bar{K}$  threshold, the deviation from zero is smaller than 1.05 times the value of the errors for the  $S_0$ -wave, smaller than 1.2 for the  $S_2$ -wave and smaller than 0.65 for the  $P$ -wave.

## 2 S, P and D waves at higher energies but below 1.42 GeV

In this section the main features of the new parametrizations of  $S$ ,  $P$  and  $D$  waves between roughly the  $K\bar{K}$  threshold and 1.42 GeV are presented. Details of each parametrization can be found in [2]. Since the description of the  $S_2$ -wave was not changed in [2], any information on this wave is available in [1].

### 2.1 The $S_0$ -wave

In the present approach we obtain both the tangent of the phase shifts  $\tan \delta_0^0$  and the inelasticity  $\eta_0^0$  above 0.932 GeV as functions of  $\mathbf{K}$ -matrix elements

$$K_{ij}(s) = \frac{\mu\alpha_i\alpha_j}{M_1^2 - s} + \frac{\mu\beta_i\beta_j}{M_2^2 - s} + \frac{1}{\mu}\gamma_{ij}, \quad (1)$$

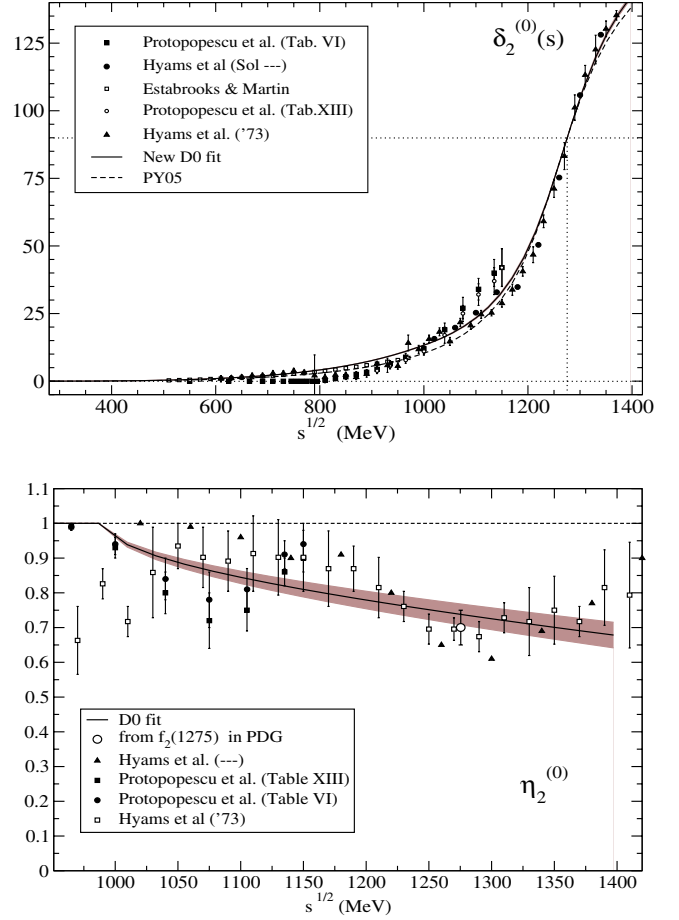


**Fig. 2.** The  $D_0$ -wave phase shifts and inelasticities determined in [2] (solid lines) and in [1] (dotted line —only for phase shifts). Dark areas denote the errors, which for the phase shifts have just the thickness of the line.

where  $i, j = 1, 2$  denote  $\pi$  or  $K$ , respectively, and we set the mass scale  $\mu = 1$  GeV. All  $\alpha_i, \beta_i$  and  $\gamma_i$  are determined from the fit. Note that  $M_1 = 0.9105 \pm 0.0070$  GeV simulates the left-hand cut of the  $\mathbf{K}$ -matrix located at  $2\sqrt{M_K^2 - m_\pi^2} = 0.952$  GeV and the pole at  $M_2 = 1.324 \pm 0.006$  GeV is connected with  $\delta_0^0$  passing through  $270^\circ$ . The parametrizations of [1] (below 0.932 GeV) and of [2] (above 0.932 GeV) are matched at 0.932 MeV. In the fit, all data on phase shifts below and above the  $K\bar{K}$  threshold [3–6] have been used simultaneously. For  $\eta_0^0$ , data from  $\pi\pi \rightarrow K\bar{K}$  have been used together with data on  $\pi\pi \rightarrow \pi\pi$  [3–7]. The resulting fit yields  $\chi^2/\text{d.o.f.} = 0.6$  and can be seen in fig. 1.

### 2.2 The $D_0$ -wave

For this wave we proceeded by fitting simultaneously below and above the  $K\bar{K}$  a parametrization

$$\cot \delta_2^{(0)} = \frac{s^{1/2}}{2k^5} (M_{f_2}^2 - s) m_\pi^2 (B_0 + B_1 w(s)) \quad (2)$$

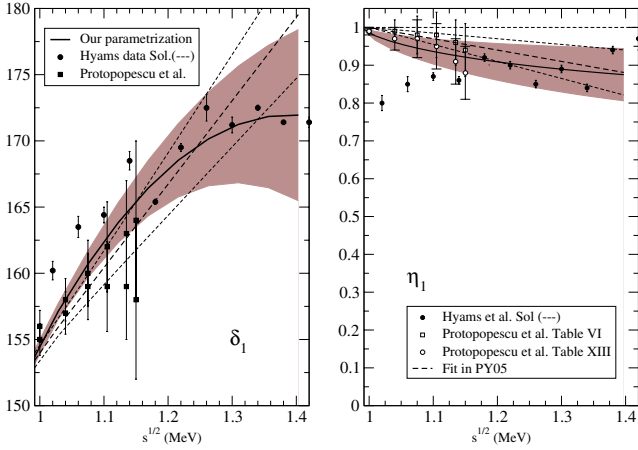


**Fig. 3.** Fits to the  $P$ -wave phase shifts and inelasticity (solid lines). Dark areas show the errors of our results. The dotted lines represent results obtained in [1].

with  $w(s) = \frac{\sqrt{s} - \sqrt{s_0 - s}}{\sqrt{s} + \sqrt{s_0 - s}}$ , but using different  $B_i$  and  $s_0$  parameters above and below  $KK$  threshold. We also required both parametrizations to match at  $\sqrt{s} = 2m_K$ , thus eliminating one parameter. In the present approach, the mass of the  $f_2(1270)$ -resonance  $M_{f_2}$  was fixed to the PDG value [9]. The  $B_i$  parameters have been obtained for those two energy regions from fits to experimental data points [3,6,8] together with three other constraints: the width of the  $f_2(1270)$ -resonance from [9], plus the scattering length and the slope parameter calculated from the Froissart-Gribov representation. The resulting  $\chi^2/\text{d.o.f.} = 0.65$ .

The inelasticity is parametrized in the same way as in [1] and fitted to the experimental data of refs. [3,6,8]

$$\eta_2^{(0)}(s) = 1 - \epsilon \frac{k_2(s)}{k_2(M_{f_2}^2)}. \quad (3)$$

Results of the fits for phase shifts and inelasticities are presented in fig. 2.

### 2.3 The $P$ -wave

In the  $P$ -wave, above the  $K\bar{K}$  threshold, we have used a more flexible parametrization than in [1]:

$$\delta_1(s) = \lambda_0 + \sum_{i=1}^2 \lambda_i \left( \sqrt{s/4m_K^2} - 1 \right)^i, \quad (4)$$

$$\eta_1(s) = 1 - \sum_{i=1}^2 \epsilon_i \left( \sqrt{1 - 4m_K^2/s} \right)^i, \quad (5)$$

where  $\lambda_0$  is fixed by the phase shift at  $2m_K$  which is obtained from the fit to the pion form factor [11]. We have then fitted data from [6,8] obtaining  $\chi^2/\text{d.o.f.} = 0.6$  and  $\chi^2/\text{d.o.f.} = 1.1$  for the phase shifts and inelasticity, respectively. The results are presented in fig. 3.

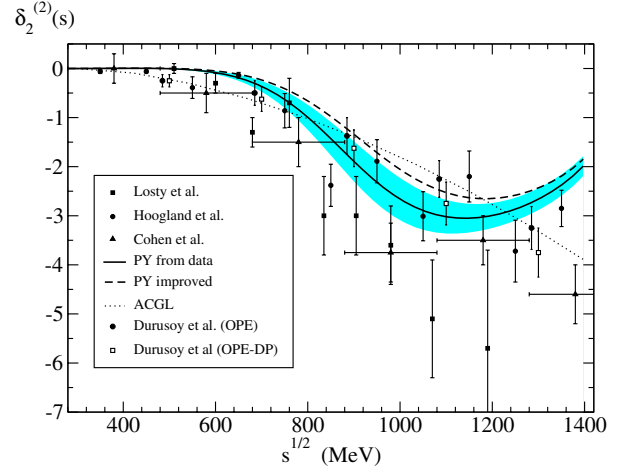


**Fig. 4.** Results of the fit to the  $D2$ -wave. The solid line denotes the fit to the experimental data only and the dashed one the fit to the data and FDR [1]. For the data enclosed in the figure see references in [2].

### 2.4 The $D2$ -wave

In the  $D2$ -wave we have used one single parametrization up to 1.42 GeV with four free parameters

$$\cot \delta_2^{(2)} = \frac{s^{1/2}}{2k^5} (B_0 + B_1 w(s) + B_1 w(s)^2) \frac{m_\pi^4 s}{4(m_\pi^2 + \Delta^2) - s}, \quad (6)$$

where  $\Delta$  fixes zero of the phase shift near the  $\pi\pi$  threshold. Since the data on this wave are not accurate we have added one more constrain using the scattering length calculated from the Froissart-Gribov representation [1]. As a result we have obtained the fit presented in fig. 4.

The lack of experimental data on inelasticity led us to estimate it from a model (see ref. [2]) writing

$$\eta_2^{(2)} = 1 - \epsilon(1 - \hat{s}/s)^3, \quad (7)$$

with  $\sqrt{\hat{s}} = 1.05$  GeV and  $\epsilon = 0.2 \pm 0.2$ . The inelasticity is very small and even negligible below 1.25 GeV.

## 3 Regge parametrization

In the analysis of [1,10] the fits were made with the assumption of “exact degeneracy” of the intercept parameters  $\alpha_\rho = \alpha_{P'}$  for  $\rho$  and  $f_2$  exchange. In our new approach this degeneracy has been lifted. As a consequence, there was a very small change in the high-energy behaviour of scattering amplitudes (especially a little for higher energies) but, as can be seen in next section, even such a small change could be significant given the level of precision achieved in our FDR calculation. The energy dependence of the new scattering amplitudes after eliminating the degeneracy is seen in fig. 5.

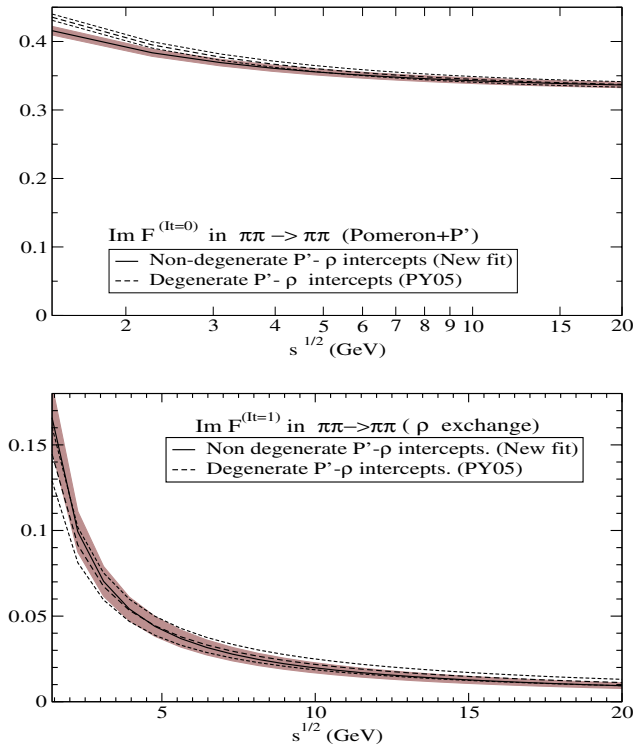


**Fig. 5.** The scattering amplitudes calculated with “exact degeneracy” (broken lines) and without this condition (solid lines). Dark bands stand for uncertainties.

#### 4 Implementation of forward dispersion relations

The  $S$ ,  $P$  and  $D$  waves presented in sect. 2 together with the improved Regge description in the previous section have been examined in the same way as in [1], by checking the FDRs, but without imposing them as constraints. Thus, in fig. 6 we present the results from the amplitudes in [1] obtained from fits to data. In contrast, in fig. 7 we show results using the improved fits given in [2], that we are reviewing here before checking that they also satisfy the Roy equations. The  $F_{00}$ ,  $F_{0+}$  and  $I_t = 1$  names used in figs. 6 and 7 correspond to the FDRs for the  $\pi^0\pi^0$ ,  $\pi^0\pi^+$  and  $t$ -channel isospin-1 scattering amplitudes, whose full mathematical expressions can be found in [1] and [2]. The word “dispersive” denotes results obtained from the integrals in the FDRs whereas “direct” means the real parts evaluated directly from parametrizations.

We provide in table 1 the FDRs averaged  $\chi^2$  obtained over the range from threshold up to 930 MeV or 1420 MeV. Note that the modifications in the  $S$  and  $P$  waves above  $KK$  threshold, as well as of the  $D$ -wave, lead to a significant improvement of the accuracy in the FDRs for the  $\pi^0\pi^0$  scattering amplitudes when compared with the previous results in [1]. The final decrease of the  $\chi^2$  for  $\pi^0\pi^+$  is also due to the influence of the new Regge amplitude. Note that in the  $I_t = 1$  case there is a tiny deterioration despite a significant  $\chi^2$  decrease due to the Regge part.

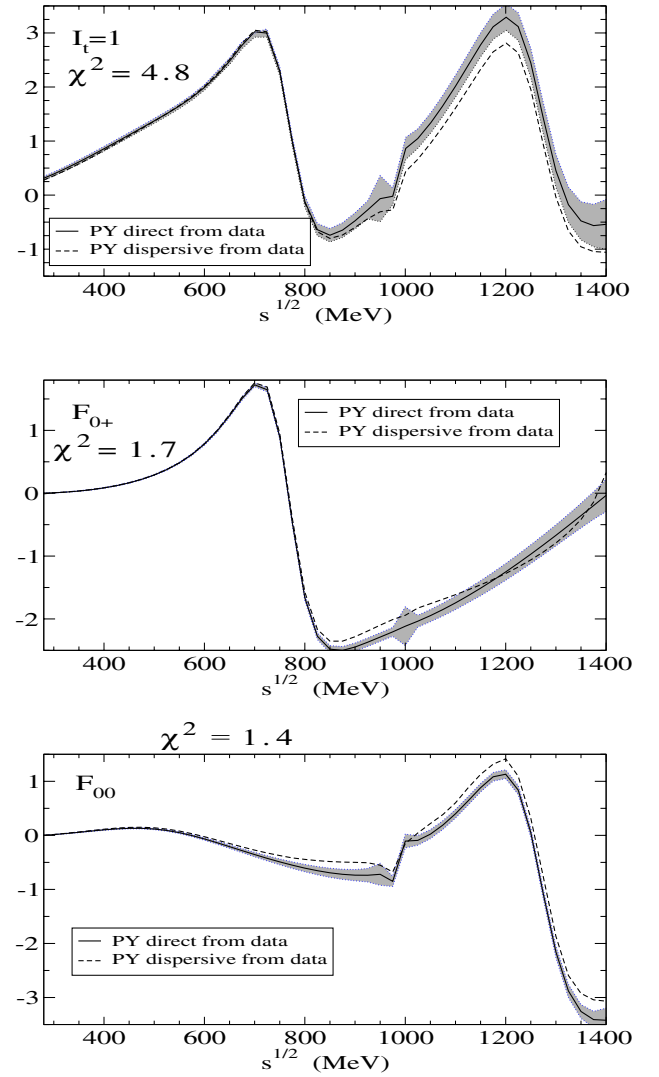


**Fig. 6.** The  $\pi^0\pi^0$ ,  $\pi^0\pi^+$  and  $t$ -channel 1 forward dispersion relations described in previous analysis [1]. The values of the  $\chi^2$  denote averaged values over all 25 points chosen in the energy range from the  $\pi\pi$  threshold to 1.42 GeV.

**Table 1.** Comparison of averaged  $\chi^2$  for different FDRs obtained in a previous analysis [1] and in the presented one (new  $\delta$ ,  $\eta$  and new Regge) in two energy ranges. Numbers correspond to fits to experimental data only (without constraints from FDRs).

Results of [1]	New $\delta, \eta$	New Regge	Energy range
For $\pi^0\pi^0$ dispersion relations			
3.8	1.52	1.41	$s^{1/2} < 930$ MeV
4.8	1.76	1.63	$s^{1/2} < 1420$ MeV
For $\pi^0\pi^+$ dispersion relations			
1.7	1.75	1.60	$s^{1/2} < 930$ MeV
1.7	1.60	1.44	$s^{1/2} < 1420$ MeV
For $I_t = 1$ scattering amplitudes			
0.2	0.57	0.32	$s^{1/2} < 930$ MeV
1.4	2.32	1.76	$s^{1/2} < 1420$ MeV

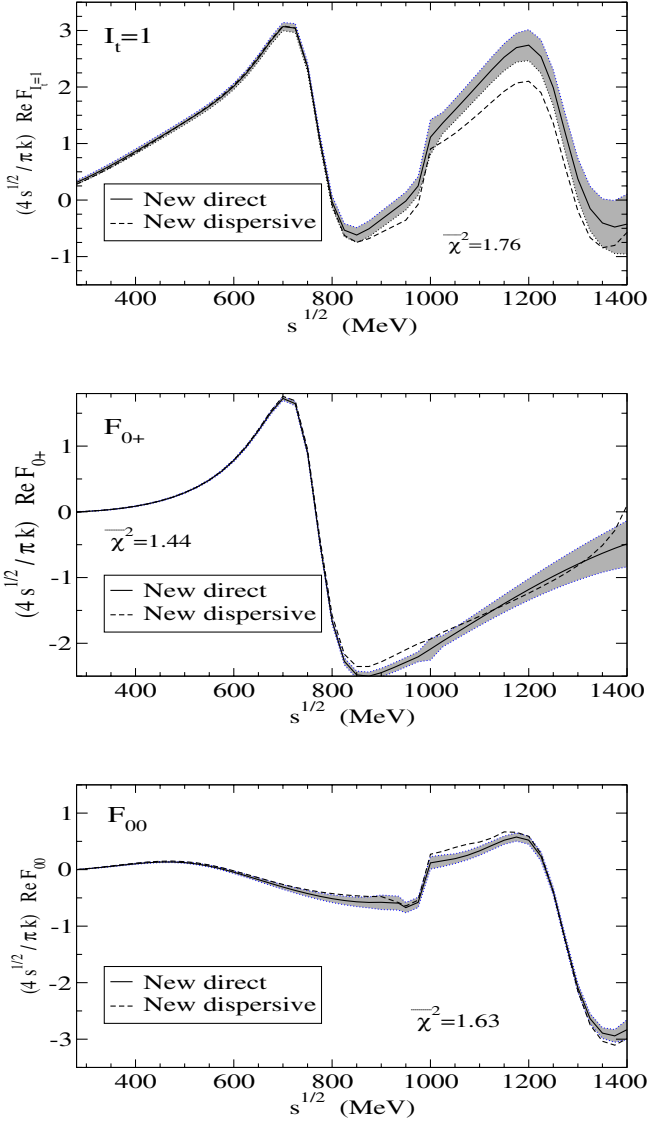


**Fig. 7.** Dispersion relations for new  $S$ ,  $P$  and  $D$  waves described in this paper. The  $\chi^2$  definition as in fig. 6.

## 5 Tests using Roy's equations

We here present an advance of our ongoing analysis where we test our new  $\pi\pi$  scattering amplitudes using Roy's equations [12–14]:

$$\begin{aligned} \text{Re } f_\ell^I(s) &= a_0^0 \delta_{I0} \delta_{\ell 0} + a_0^2 \delta_{I2} \delta_{\ell 0} \\ &+ (2a_0^0 - 5a_0^2) \left( \delta_{I0} \delta_{\ell 0} + \frac{1}{6} \delta_{I1} \delta_{\ell 1} - \frac{1}{2} \delta_{I2} \delta_{\ell 0} \right) \frac{s - 4\mu^2}{12\mu^2} \\ &+ \sum_{I'=0}^2 \sum_{\ell'=0}^1 \int_{4\mu^2}^{s_{max}} ds' K_{\ell\ell'}^{II'}(s, s') \text{Im } f_{\ell'}^{I'}(s') \\ &+ d_\ell^I(s, s_{max}), \end{aligned} \quad (8)$$

where

$$f_\ell^I(s) = \sqrt{\frac{s}{s - 4\mu^2}} \frac{1}{2i} \left( \eta_\ell^I e^{2i\delta_\ell^I} - 1 \right), \quad (9)$$

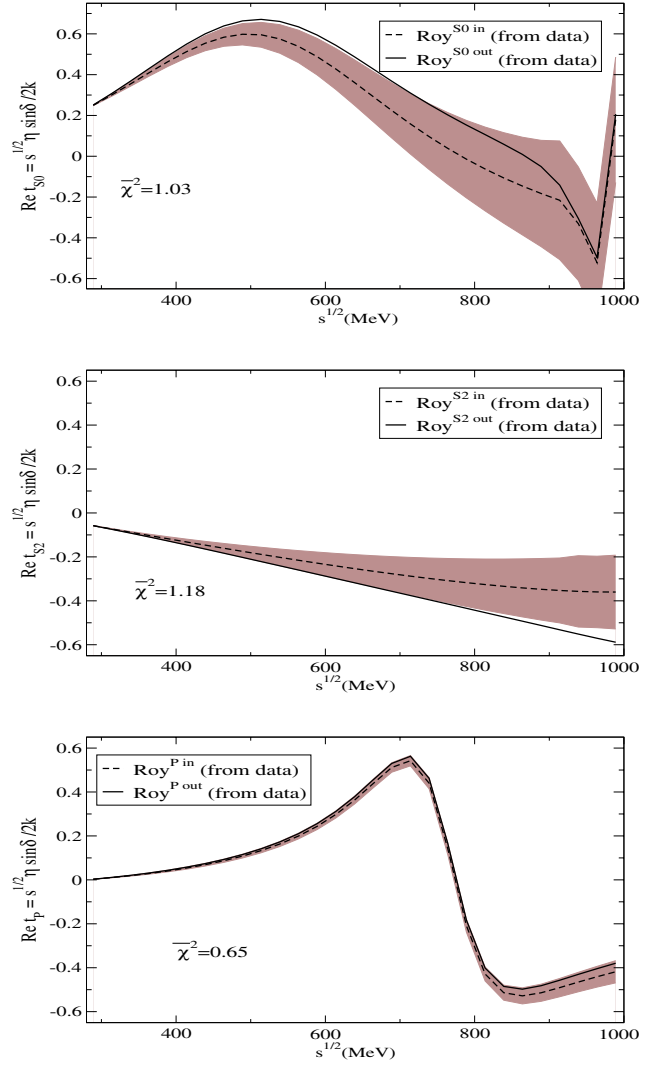


**Fig. 8.** Differences between real parts of amplitudes calculated directly from amplitudes and those from the integral representation of Roy's equations. The notation is explained in the sect. 5.

with  $a_0^0$  and  $a_0^2$  being the  $S0$  and  $S2$  scattering lengths,  $K_{\ell\ell'}^{II'}(s, s')$  known kernels and  $d_\ell^I(s, s_{max})$  the so-called driving terms. In our calculations we have chosen  $s_{max} = 103m_\pi^2$ .

In fig. 8 we show the real part of the  $S0$ ,  $S2$  and  $P$  partial waves obtained from eq. (8) (continuous line, called  $\text{Roy}^{out}$ ) versus the real part obtained directly from our parametrizations (dashed line, called  $\text{Roy}^{in}$ ).

The agreement is remarkable, taking into account the uncertainties (the dark areas in fig. 8). Furthermore, the agreement is even more impressive, taking into account that we have not imposed any constraints from FDRs or Roy's equations themselves and that the amplitudes come just from fits to data (that is why they are labeled “from data” in the figure). Moreover, we use the new  $S$ ,  $P$  and  $D$  waves described in sect. 2 and the Regge model with different intercepts  $\alpha_\rho(0)$  and  $\alpha_{\rho'}(0)$ , and all of them have experimental errors even smaller than those of [1].

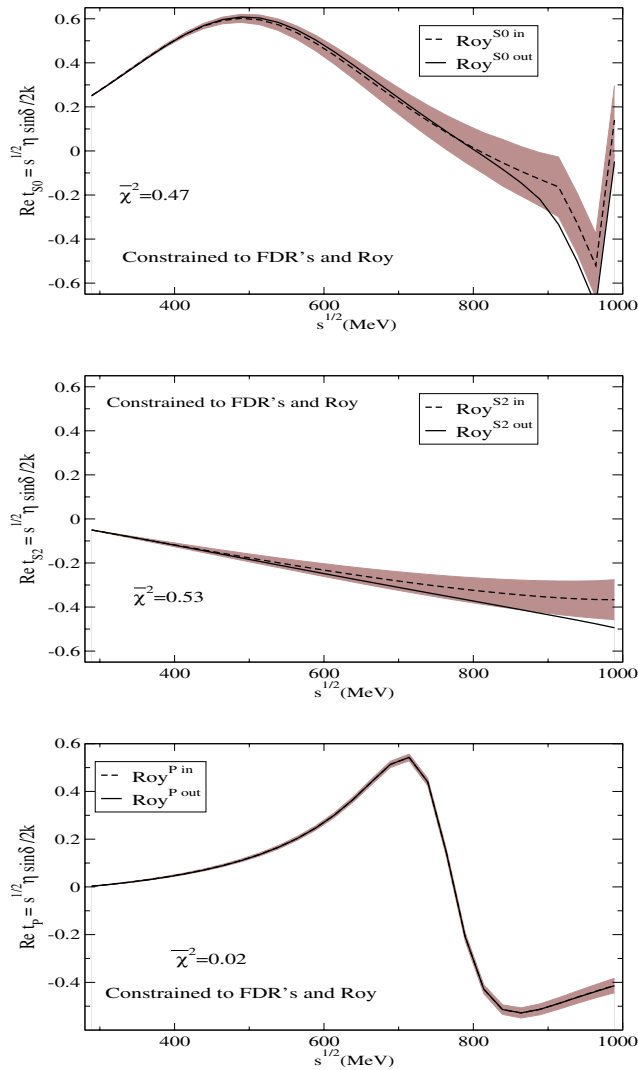


**Fig. 9.** As in fig. 8 but for data fits constrained by FDRs and Roy's equations.

## 6 Conclusions

The results reviewed here indicate that the improvement in the fits to data in the  $S$  and  $P$  waves above  $KK$  threshold and the  $D$ -wave described in sect. 2 together with a slight improvement in Regge trajectories, allowing for non  $\rho - f$  degeneracy, also improves the fulfillment of forward dispersion relations. Despite the smaller errors of those amplitudes, the averaged  $\chi^2$  is indeed lower than in previous analysis [1].

But also here, as the main novelty, we have shown that those amplitudes fulfill also quite well Roy's equations, and therefore, crossing symmetry, up to roughly 1 GeV.

Following, however, the analysis done in [1] one can think about a wider implementation of FDR including them into the fits together with the already fitted experimental data. We report briefly on our progress in this approach, where, for the moment, we allow for a variation of all the amplitude parameters except, the  $P$ -wave above  $KK$  threshold and just the  $\alpha$  and  $\beta$  parameters in the  $\mathbf{K}$ -matrix. Although our results are just preliminary, we already noticed significant decreases of the averaged  $\chi^2$  for all three FDRs. The preliminary values for  $F_{00}$  decreased from 1.63 to 0.42, for  $F_{0+}$  changed slightly from 1.44 to 1.48 and for  $I_t = 1$  decreased from 1.76 to 0.89. The more spectacular improvement, however, has been noticed in the Roy equations. Preliminary averaged  $\chi^2$  values decreased from 1.03 to 0.47 for the  $S0$ -wave, from 1.18 to 0.53 for the  $S2$ -wave and from 0.65 to 0.02 for the  $P$ -wave. This improvement can be clearly seen when comparing figs. 8 and 9. Imposing the constrains from Roy equations and particularly from FDRs, which is much stringent, leads to modifications in the  $S$ ,  $P$  and  $D$  waves by less than  $1\sigma$  (with the exception for  $D2$ -wave where the empirical fit changed by  $\sim 1.3\sigma$ ) and to negligible modifications in all other waves. The resulting uncertainties are also significantly reduced with this approach as can be seen, just for Roy equations, in figs. 8 and 9. At present we are finishing the determination of the final parameters and their uncertainties.

## References

1. J.R. Peláez, F.J. Ynduráin, Phys. Rev. D **71**, 074016 (2005).
2. R. Kamiński, J.R. Peláez, F.J. Ynduráin, Phys. Rev. D **74**, 014001 (2006); 079903 (2006)(E).
3. B. Hyams *et al.*, Nucl. Phys. B **64**, 134 (1973); P. Estabrooks, A.D. Martin, Nucl. Phys. B **79**, 301 (1974).
4. G. Grayer *et al.*, Nucl. Phys. B **75**, 189 (1974).
5. R. Kamiński, L. Leśniak, K. Rybicki, Z. Phys. C **74**, 79 (1997); EPJdirect C **4**, 4 (2002).
6. B. Hyams *et al.*, Nucl. Phys. B **100**, 205 (1975).
7. W. Wetzel *et al.*, Nucl. Phys. B **115**, 208 (1976); D. Cohen *et al.*, Phys. Rev. D **22**, 2595 (1980); E. Etkin *et al.*, Phys. Rev. D **25**, 1786 (1982).
8. S.D. Protopopescu *et al.*, Phys. Rev. D **7**, 1279 (1973).
9. S. Eidelman *et al.*, Phys. Lett. B **592**, 1 (2004).
10. J.R. Peláez, F.J. Ynduráin, Phys. Rev. D **69**, 114001 (2004).
11. J.F. de Trocóniz, F.J. Ynduráin, Phys. Rev. D **65**, 093001 (2002); **71**, 073008 (2005).
12. S.M. Roy, Phys. Lett. B **36**, 353 (1971).
13. B. Ananthanarayan, G. Colangelo, J. Gasser, H. Leutwyler, Phys. Rep. **353**, 207 (2001).
14. R. Kamiński, L. Leśniak, B. Loiseau, Phys. Lett. B **551**, 241 (2003).